Analytical Biochemistry 436 (2013) 69–74

Contents lists available at SciVerse ScienceDirect

Analytical Biochemistry

journal homepage: www.elsevier.com/locate/yabio

# Cerium oxide–graphene as the matrix for cholesterol sensor

Meihe Zhang, Ruo Yuan *, Yaqin Chai, Cun Wang, Xiaoping Wu

*Education Ministry Key Laboratory on Luminescence and Real-Time Analysis, College of Chemistry and Chemical Engineering, Southwest University, Chongqing 400715, People's Republic of China*

ARTICLE INFO

*Article history:*
Received 20 October 2012
Received in revised form 15 January 2013
Accepted 22 January 2013
Available online 1 February 2013

*Keywords:*
Electrogenerated chemiluminescence
Graphene
Luminol
Cerium oxide
Cholesterol biosensor

ABSTRACT

A simple and sensitive electrogenerated chemiluminescence (ECL) cholesterol biosensor was prepared based on cerium oxide–graphene ($CeO_2$–graphene) composites as an efficient matrix. $CeO_2$–graphene composites were prepared by depositing $CeO_2$ onto graphene and were characterized by scanning electron microscopy. The experimental results demonstrated that $CeO_2$–graphene could catalyze the ECL of a luminol–$H_2O_2$ (hydrogen peroxide) system to amplify the luminol ECL signal greatly. In addition, the use of $CeO_2$–graphene provided a better biocompatible microenvironment for the immobilized enzyme, resulting in excellent stability and a long lifetime of the ECL biosensor. The surface assembly process, ECL behaviors, and electrochemistry of the biosensor were investigated in detail. The quantity of cholesterol was in the linear range from 12 μM to 7.2 mM with a detection limit of 4.0 μM (signal/noise = 3). In addition, the biosensor exhibited outstanding reproducibility, long-term stability, and selectivity. Moreover, this cholesterol biosensor offers an alternative analytical method with low cost and high speed.



Recently, fast and accurate determination of cholesterol has aroused much attention because it is closely associated with the diagnosis of coronary heart diseases, hypertension, and lipid metabolism dysfunction [1,2]. Up to now, several methods have been used for clinical serum sample measurements [3,4]. However, there is still a critical demand for rapid, simple, sensitive, and low-cost detection technologies for detection of cholesterol, especially in point-of-care applications. Electrogenerated chemiluminescence (ECL),[1] involving a light emission process in a redox reaction of electrogenerated reactants, combines electrochemical and luminescent techniques [5,6]. Owing to its high sensitivity and wide dynamic concentration response range, ECL is an important and valuable detection method in analytical chemistry and has been used for cholesterol determination [7].

Luminol (5-amino-2,3-dihydro-1,4-phthalazinedione) produces strong ECL at a wavelength of 425 nm under appropriate experimental conditions [8,9]. However, in a luminol ECL system, an alkaline medium (pH 10.0–12.0) should be afforded, limiting the use of an ECL biosensor. To improve sensitivity and selectivity, much attention has been extended to ECL systems. As we know, luminol can be oxidized by hydrogen peroxide ($H_2O_2$), and this oxidized process can be catalyzed by transition metal ions such as Co(II), Cu(II), and Fe(III) as well as some metallocomplexes (hemin and peroxidases) [10–12]. Especially, metal nanoparticles used as catalysts in ECL reactions have provided new approaches to enhance sensitivity and expand new applications of this mode of detection. Gold nanoparticles and platinum nanoparticles efficiently promoting the ECL of luminol have been reported [13,14]. Recently, some metal oxide photocatalysts have been suggested as highly photosensitive photocatalysts to improve photocatalytic activity. For example, ZnO nanoparticles were found to directly enhance the chemiluminescence of a luminol–$H_2O_2$ system [15].

During recent years, rare earth oxides have drawn tremendous interest in both theoretical and technological fields. Especially, cerium oxide ($CeO_2$), owing to its biocompatibility, high isoelectric point (IEP), mechanical strength, and excellent adsorption capability, is attractive with extensive applications such as gas sensors and photocatalytic oxidation of water [16]. Furthermore, due to the high surface-to-volume ratio, $CeO_2$ has a high capacity to absorb molecules such as proteins, amino acids, and sugars. Owing to its high IEP (~9.0), $CeO_2$ is suitable for adsorption of enzymes with low IEP (e.g., glucose oxidase with an IEP of 4.2) without any harsh chemical treatment [17]. Furthermore, $CeO_2$ can exhibit catalase mimetic activity and can convert $H_2O_2$ to water and molecular oxygen. More important, polyacrylic acid-coated nanoceria can enhance the ECL intensity of the luminol–$H_2O_2$ system [18].

Graphene, emerging as a true two-dimensional structure of carbon atoms, has received a great deal of attention because of its unique thermal, electronic, and mechanical properties. Due to

* Corresponding author. Fax: +86 23 68253172.
*E-mail address:* yuanruo@swu.edu.cn (R. Yuan).

[1] *Abbreviations used:* ECL, electrogenerated chemiluminescence; $H_2O_2$, hydrogen peroxide; $CeO_2$, cerium oxide; IEP, isoelectric point; GCE, glassy carbon electrode; ChOx, cholesterol oxidase; CS, chitosan; PBS, phosphate buffer solution; CV, cyclic voltammetry; SEM, scanning electron microscopy; AFM, atomic force microscopy; FT-IR, Fourier transform infrared; RMS, root mean square.

0003-2697/$ - see front matter © 2013 Elsevier Inc. All rights reserved.
http://dx.doi.org/10.1016/j.ab.2013.01.022

the unique physical and chemical properties of graphene, such as high surface area, excellent conductivity, and ease of functionalization and production, graphene provides an ideal base for electric devices, electronics, and biosensors. Specifically, electronic properties of graphene have been altered by electrochemical modification and chemical functionalization. Meanwhile, numerous hybrids, such as graphene/Pt nanoparticle sheets and graphene/metal oxide deposits, have been reported [19,20]. So far, only a few studies have been aimed at producing graphene-supported $CeO_2$ ($CeO_2$–graphene).

On the basis of the findings, we designed an ECL biosensor based on $CeO_2$–graphene for detection of cholesterol. Here, $CeO_2$–graphene composites were synthesized in aqueous solution and were modified onto a bare glassy carbon electrode (GCE). The $CeO_2$–graphene composites combine the excellent electrocatalytic activity of $CeO_2$ toward $H_2O_2$ that performs a catalytic property to amplify the luminol ECL signal greatly and more excellent electrical conductivity owing to the ability to promote the electron transfer and increase the ECL intensity of the luminol–$H_2O_2$ system of the graphene together. Because both $CeO_2$ and graphene are promising matrices for enzyme immobilization, cholesterol oxidase (ChOx) was adsorbed on the surface of $CeO_2$–graphene composites to construct a cholesterol biosensor. The catalytic activity of $CeO_2$–graphene for luminol ECL was investigated in detail. $CeO_2$–graphene exhibited good performance in terms of sensitivity and catalytic activities. Furthermore, the biosensor showed satisfying performance toward cholesterol detection.

## Materials and methods

### Chemicals

Graphene, $Ce(NO_3)_3{\cdot}6H_2O$, ChOx (EC 1.1.3.6, $\geqslant$50 U/mg, form *Brevibacterium* sp.), cholesterol ($C_{27}H_{46}O$, $M_r$ = 386.67, $\geqslant$99% purity, form lanolin), Triton X-100 ($C_{34}H_{62}O_{11}$, MW = 646.85), and chitosan (CS, MW = 100,000–300,000, deacetylating grade = 70–85%, from crab shells) were obtained from Sigma Chemical (St. Louis, MO, USA). Phosphate buffer solutions (PBSs, containing 0.9% NaCl, pH 7.4) were prepared with 0.05 M $KH_2PO_4$ and 0.05 M $Na_2HPO_4$. The stock solution was prepared by dissolving cholesterol in a mixture of 2-propanol and Triton X-100 and then diluting it only with Triton X-100 solution for preparing standard solutions. $K_3[Fe(CN)_6]$ and other chemicals used were of analytical grade and were used as received. Double distilled water was used throughout this study.

### Apparatus

Cyclic voltammetry (CV) was performed with a CHI 600D electrochemical workstation (Shanghai CH Instruments, China). The ECL emission was monitored with a model MPI-A electrochemiluminescence analyzer (Xi'an Remax Electronic Science and Technology, China), with the voltage of the photomultiplier tube (PMT) set at 600 V during the process of detection. All experiments were performed with a conventional three-electrode system: the modified GCE as working electrode, a platinum wire as counter electrode, and a saturated calomel electrode (SCE) or Ag/AgCl (saturated KCl) as reference electrode. The images of $CeO_2$–graphene composites were characterized by scanning electron microscopy (SEM, S-4800, Hitachi, Japan). The images of the stepwise assembly processes of the electrode were characterized by atomic force microscopy (AFM, Veeco, Woodbury, NY, USA). The Fourier transform infrared (FT-IR) spectra were recorded on a Nexus 670 FT-IR spectrophotometer (Nicolet Instruments) using KBr pellets.

### Synthesis of $CeO_2$–graphene

The $CeO_2$–graphene composites were synthesized according to the literature [21]. $CeO_2$ was deposited onto the graphene material dropwise, adding 5 M KOH solution into a beaker containing graphene and $Ce(NO_3)_3$ aqueous solution under stirring until the cerium ions precipitated completely. After filtering, the residue was aged for 30 min in air and then washed repeatedly with water, followed by drying at 100 °C. SEM was employed to observe the prepared composites. As shown in Fig. 1B, the $CeO_2$ appeared randomly on the basal planes of the graphene nanosheets, which was different from that on graphene nanosheets (Fig. 1A), indicating that $CeO_2$–graphene composites were synthesized successfully. FT-IR was employed to further investigate the structure of the $CeO_2$–graphene composites shown in Fig. S1 (see Supplementary material). The $CeO_2$–graphene composites were dispersed in CS solution (1 mg $ml^{-1}$ in 1% HAc) for future use.

### Fabrication process and detection principle of biosensor

Scheme 1 shows the schematic diagram of fabrication of the cholesterol biosensor. The GCE ($\Phi$ = 4 mm) was first polished to a mirror-like surface repeatedly with 0.3 and 0.05 μm alumina slurry, followed by successive sonication in bidistilled water and ethanol for 5 min and drying in air. Subsequently, 10 μl of $CeO_2$–graphene composites was dropped onto the surface of the bare GCE. After drying in air, 6 μl of ChOx solutions (1 mg $ml^{-1}$ in 0.1 M PBS, pH 7.0) was dropped onto the surface of the electrode to construct a cholesterol biosensor (denoted as ChOx/$CeO_2$–graphene/GCE). For comparison, ChOx/graphene/GCE was prepared similarly. The modified electrodes were stored at 4 °C for future use.

The major ECL mechanism for the luminol–$H_2O_2$ system has been summarized. On the basis of previously reported results and those obtained in this study for the luminol–$H_2O_2$ ECL system, it is proposed that various reactive oxygen species (not shown in Scheme 1) are produced from $H_2O_2$ and that luminol is oxidized to the luminol radical anion. The subsequent chemical reaction of luminol radical anions with reactive oxygen species creates the ECL signal. In this study, $CeO_2$–graphene can significantly enhance the ECL signal by increasing the amount of various electrogenerated reactive oxygen species from the $H_2O_2$. As shown in Scheme 1, ChOx catalyzed the oxidation of cholesterol to produce $H_2O_2$. Under positive potential, with the help of $CeO_2$–graphene, the luminol produced stronger ECL signals. The intensity of the ECL signal was directly proportional to the concentration of cholesterol. So, cholesterol can be detected quantitatively on the modified electrode.

## Results and discussion

### Characterization of biosensor fabrication

The AFM technique was employed to confirm the fabrication process of the biosensor. AFM images of Au substrate modified with different materials are shown in Fig. 1. AFM image of $CeO_2$–graphene revealed the formation of rough surface morphology with uniformly distributed nanopores and the presence of a globular microstructure (Fig. 1C). The image of $CeO_2$–graphene film presented a homogeneous surface, and its root mean square (RMS) roughness was 123.08 nm. After ChOx was adsorbed on the $CeO_2$–graphene (Fig. 1D), the surface of the ChOx/$CeO_2$–graphene layer exhibited a smoothing effect as compared with that of the $CeO_2$–graphene layer (RMS = 91.692 nm). The globular structure disappeared and the random cloud-like structure could be seen, indicating that the ChOx was successfully absorbed on the $CeO_2$–graphene layer.

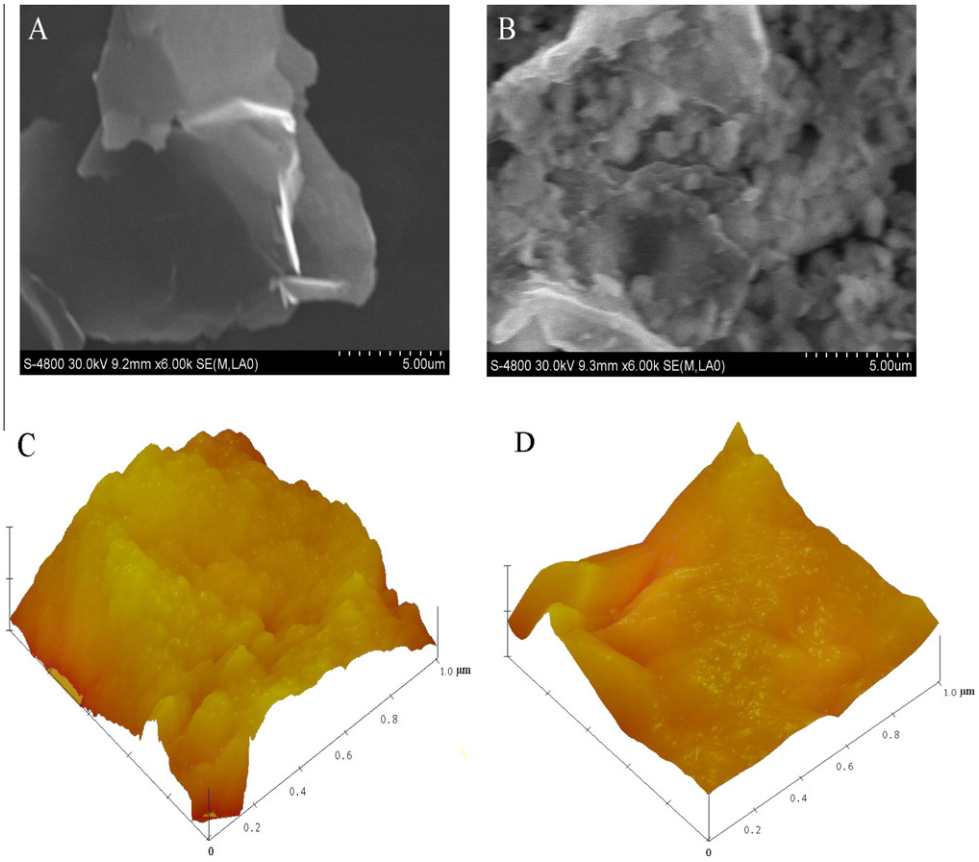


**Fig.1.** (A and B) SEM images of graphene (A) and $CeO_2$–graphene (B). (C and D) AFM images of different modified Au substrates: $CeO_2$–graphene/Au (C) and ChOx/$CeO_2$–graphene/Au (D).

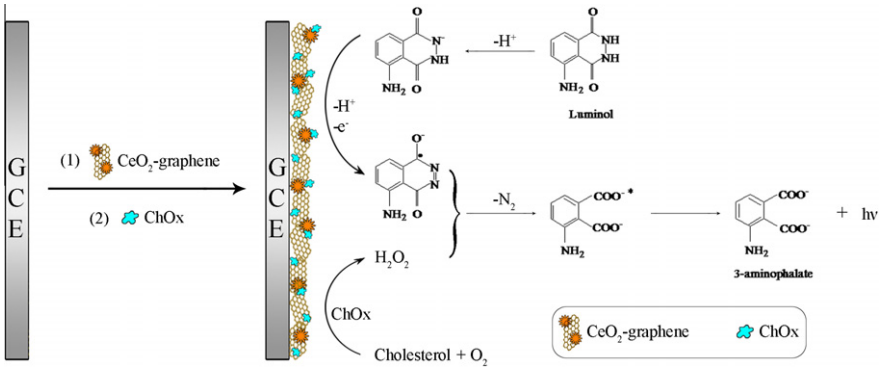


**Scheme 1.** Illustration of fabrication process and detection principle of the biosensor.

CV is also a convenient and valuable technology to monitor the characteristics of the process of electrode modification. Cyclic voltammograms of different modified electrodes in 5 mM $Fe(CN)_6^{4-/3-}$ solution (0.1 M KCl) are shown in Fig. S2 of the Supplementary material. As can be seen, a well-defined oxidation and reduction peak of $[Fe(CN)_6]^{4-/3-}$ (curve a) was observed at the bare GCE. After the $CeO_2$–graphene was modified on the surface of GCE, the peak current of the modified electrode increased (curve b). The reason for this is that $CeO_2$–graphene composites have an excellent electrotransfer property that accelerated the transfer electrons toward the electrode surface, indicating that the $CeO_2$–graphene had been immobilized successfully. However, when ChOx was adsorbed on the surface of the $CeO_2$–graphene composites, the peak current decreased markedly (curve c) for the hindrance of nonconductive ChOx.

*Optimization of analytical conditions*

To optimize the performance of the prepared ECL biosensor toward cholesterol detection, the effect of the concentration of luminol on the ECL intensity was examined. The ECL intensity increased with increasing luminol concentrations (Fig. 2A). A further increase in the concentration of luminol (from 0.15 to 0.50 mM) did not cause obvious enhancement of the intensity of the ECL. Consider-

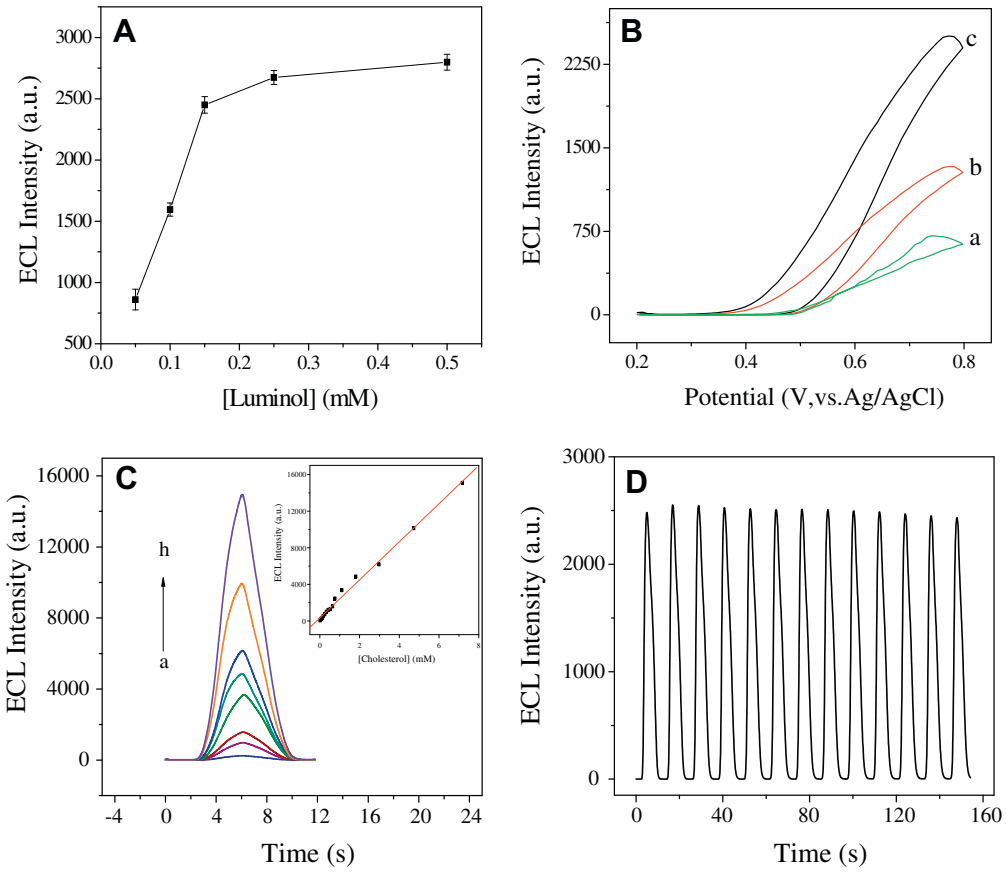


**Fig.2.** (A) Effect of luminol concentration on ECL responses to cholesterol at ChOx/$CeO_2$–graphene/GCE. (B) ECL responses of luminol (0.15 mM) at ChOx/$CeO_2$/GCE (a), ChOx/graphene/GCE (b), and ChOx/$CeO_2$–graphene/GCE (c) to 0.85 mM cholesterol. (C) ECL responses of luminol (0.15 mM) at ChOx/$CeO_2$–graphene/GCE in the presence of 0.07 (a), 0.33 (b), 0.64 (c), 1.1 (d), 1.8 (e), 3.0 (f), 4.7 (g), and 7.2 (h) mM cholesterol. The inset shows the linear relationship between the ECL signal intensity and the concentration of cholesterol. (D) Reproducibility of ECL responses of luminol (0.15 mM) at ChOx/$CeO_2$–graphene/GCE. Condition: 0.05 M PBS (pH 7.4); scan rate: 100 mV $s^{-1}$.

ing the ECL intensity and the consumption of the reagents, 0.15 mM was selected as the optimal concentration of luminol in this work.

*Performance of biosensor*

To explore the effect of graphene, $CeO_2$, and $CeO_2$–graphene on the intensity of the ECL signal of the biosensor, a comparative study was carried out by using three kinds of biosensors: (i) ChOx/$CeO_2$/GCE, (ii) ChOx/graphene/GCE, and (iii) ChOx/$CeO_2$–graphene/GCE. The ECL intensity of luminol was enhanced to a much greater extent in the presence of $CeO_2$–graphene (Fig. 2B). It may be attributed to the electrocatalytic properties of $CeO_2$–graphene; more efficient active sites were created for the catalytic oxidation of $H_2O_2$ to produce various reactive oxygen species that can enhance the ECL intensity of luminol. Furthermore, $CeO_2$ was potent free radical scavengers with the unique property of being regenerative or autocatalytic at physiological pH values.

The analytical applicability of the prepared biosensor for ECL determination of cholesterol was explored at the optimized conditions by detecting standard cholesterol solutions. The ECL intensity of luminol was found to increase with the increasing concentrations of cholesterol. Fig. 2C reveals the ECL behaviors of the biosensor at determining cholesterol, and the calibration graph of the intensity of ECL versus cholesterol concentration was in the linear range from 12 μM to 7.2 mM with a limit of detection of 4 μM (signal/noise [S/N] = 3). The regression equation was $I$ (a.u.) = $2.08 \times 10^3$ $C$ (mM) + 325 with a correlation coefficient of 0.993. The current luminol ECL detection method showed good reproducibility in the determination of cholesterol. The relative standard deviation (RSD) for repetitive measurements ($n$ = 11) of the biosensor response to 1.0 mM cholesterol (Fig. 2D) was 6.8%. The analytical features of some reported cholesterol sensors using modified electrodes with different modification strategies are summarized in Table 1. We can see that the biosensor established in this work had a low detection limit and a wide linear range, suggesting that the prepared biosensor has its advantages compared with other biosensors, which may be attributed to the greatly enhanced ECL signal using in situ generated $H_2O_2$ as a coreactant for luminol under the catalysis by $CeO_2$–graphene.

The stability of the biosensor was also tested by monitoring its ECL response to cholesterol. It was found that the response of the biosensor to 1.0 mM cholesterol decreased 19.8% after 2 weeks. The selectivity and anti-interference ability of the biosensor were investigated by analyzing a standard solution of 1.0 mM cholesterol in existing interfering species. The interfering species, such as urea (10 mM), uric acid (10 mM), glycine (10 mM), and ethanol (10 mM), did not cause any observable interference to the response to cholesterol, indicating that the prepared biosensor showed high selectivity and good anti-interference ability.

*Recovery experiment*

To evaluate the performance of the prepared ECL biosensor, several different concentrations of standard cholesterol solution were determined by using the developed biosensor with the standard addition method. A part of the experimental results is shown in Table 2. The recovery was from 94.2 to 105.2%, indicating that

**Table 1**
Comparison of some of the response characteristics of the different modified electrodes for the determination of cholesterol.

| Electrode material | Determination method | Linear range (μM) | Detection limit (μM) | References |
|---|---|---|---|---|
| ChOx/p(pyrrole)[a]/p(HEMA)[b] | Chronoamperometry | 500–1500 | 120 | [22] |
| ChOx–Chi[c]/Hb[d]–Chi/GCE | Chronoamperometry | 10–600 | 9.5 | [23] |
| ChOx/Chi–IL[e]/MWNT[f](SH)–Au | Chronoamperometry | 500–5000 | – | [24] |
| ([ChOx–MWNT]$_5$–PDDA[g])/Gr | CV | 200–1000 | 30 | [25] |
| ChOx/$CeO_2$–graphene/GCE | ECL | 12–7200 | 4.0 | This work |

[a] p(pyrrole), polypyrrole.
[b] p(HEMA), poly(2-hydroxyethyl methacrylate).
[c] Chi, chitosan.
[d] Hb, hemoglobin.
[e] IL, ionic liquid.
[f] MWNT, multiwall carbon nanotubes.
[g] PDDA, poly(diallyldimethylammonium chloride).

**Table 2**
Application of the biosensor for determination of the recovery of cholesterol.

| Sample | $C_{Original}$ (mM) | $C_{Added}$ (mM) | $C_{Detected}$ (mM) | Recovery (%) |
|---|---|---|---|---|
| 1 | 0.04 | 0.08 | 0.113 | 94.2 |
| 2 | 0.25 | 0.20 | 0.452 | 100.4 |
| 3 | 0.35 | 0.25 | 0.631 | 105.2 |

the proposed biosensor represented good recovery. These results demonstrated that the prepared $CeO_2$–graphene-based ECL biosensor was comparable to the clinical assay, exhibiting great promise as a reliable technique for the detection of cholesterol in practical applications.

## Conclusions

$CeO_2$–graphene composites were developed for fabrication of an ECL biosensor for the determination of cholesterol. The strong ECL emission of luminol was obtained in a neutral aqueous solution of PBS at pH 7.4. Amplification of the luminol ECL signals was achieved because of the following reasons. First, the excellent electrocatalytic activity of $CeO_2$ toward $H_2O_2$ performed a catalytic property to amplify the luminol ECL signal greatly. Second, graphene had more excellent electrical conductivity owing to the ability to promote the electron transfer and increase the ECL intensity of the luminol–$H_2O_2$ system. Third, the attached ChOx kept good biological activity and exhibited efficient catalysis toward cholesterol to generate $H_2O_2$ as a coreactant for luminol. In addition, the ECL detection method based on the $CeO_2$–graphene composites could be preferably used as a transduction method for the development of the ECL biosensor based on $H_2O_2$-liberating oxidase enzymes and ECL immunoassays using the labels of luminol derivatives or enzymes.

## Acknowledgments

This work was supported by the National Natural Science Foundation of China (21075100), the Ministry of Education of China (project 708073), the Nature Science Foundation of Chongqing City (CSTC-2011BA7003 and CSTC-2009BA1003), Specialized Research Funds for the Doctoral Program of Higher Education (20100182110015), and Fundamental Research Funds for the Central Universities (XDJK2012A004).

## Appendix A. Supplementary material

Supplementary material associated with this article can be found, in the online version, at http://dx.doi.org/10.1016/j.ab.2013.01.022.

## References

[1] N. Ruecha, W. Siangproh, O. Chailapakul, A fast and highly sensitive detection of cholesterol using polymer microfluidic devices and amperometric system, Talanta 84 (2011) 1323–1328.
[2] C.Y. Wang, X.R. Tan, S.H. Chen, R. Yuan, F.X. Hu, D.H. Yuan, Highly-sensitive cholesterol biosensor based on platinum–gold hybrid functionalized ZnO nanorods, Talanta 94 (2012) 263–270.
[3] E.M.I.M. Ekanayake, D.M.G. Preethichandra, K. Kaneto, Polypyrrole nanotube array sensor for enhanced adsorption of glucose oxidase in glucose biosensors, Biosens. Bioelectron. 23 (2007) 107–113.
[4] X.R. Li, J.J. Xu, H.Y. Chen, Potassium-doped carbon nanotubes toward the direct electrochemistry of cholesterol oxidase and its application in highly sensitive cholesterol biosensor, Electrochim. Acta 56 (2011) 9378–9385.
[5] Y. Li, H.L. Qi, Y.G. Peng, J. Yang, C.X. Zhang, Electrogenerated chemiluminescence aptamer-based biosensor for the determination of cocaine, Electrochem. Commun. 9 (2007) 2571–2575.
[6] M.M. Richter, Electrochemiluminescence (ECL), Chem. Rev. 104 (2004) 3003–3036.
[7] X.Q. Liu, L.H. Shi, H.J. Li, W.X. Niu, G.B. Xu, Tris(2,2′-bipyridyl)ruthenium(II) electrochemiluminescent detection of coreactants containing aromatic diol group by the interaction between diol and borate anion, Electrochem. Commun. 9 (2007) 2666–2670.
[8] Z.H. Wang, F. Liu, X. Teng, C.X. Zhao, C. Lu, Detection of hydrogen peroxide in rainwater based on Mg–Al–carbonate layered double hydroxides-catalyzed luminol chemiluminescence, Analyst 136 (2011) 4986–4990.
[9] Z.M. Yu, X.H. Wei, J.L. Yan, Y.F. Tu, Intensification of electrochemiluminescence of luminol on $TiO_2$ supported Au atomic cluster nano-hybrid modified electrode, Analyst 137 (2012) 1922–1929.
[10] Y.Y. Su, J. Wang, G.N. Chen, Study on the enhancement of electrochemiluminescence of luminol–$H_2O_2$ system by sulphonated cobalt(II) phthalocyanine, Anal. Chim. Acta 551 (2005) 79–84.
[11] C. Dodeigne, L. Thunus, R. Lejeune, Chemiluminescence as diagnostic tool: a review, Talanta 51 (2000) 415–439.
[12] C.A. Marquette, L.J. Blum, Applications of the luminol chemiluminescent reaction in analytical chemistry, Anal. Bioanal. Chem. 385 (2006) 546–554.
[13] H. Cui, Y. Xu, Z.F. Zhang, Multichannel electrochemiluminescence of luminol in neutral and alkaline aqueous solutions on a gold nanoparticle self-assembled electrode, Anal. Chem. 76 (2004) 4002–4010.
[14] J.Z. Guo, H. Cui, W. Zhou, W. Wang, Ag nanoparticle-catalyzed chemiluminescent reaction between luminol and hydrogen peroxide, J. Photochem. Photobiol. A 193 (2008) 89–96.
[15] S.F. Li, X.M. Zhang, W.X. Du, Y.H. Ni, X.W. Wei, Chemiluminescence reactions of a luminol system catalyzed by ZnO nanoparticles, J. Phys. Chem. C 113 (2009) 1046–1051.
[16] A. Mehta, S. Patil, H. Bang, H.J. Cho, S. Seal, A novel multivalent nanomaterial based hydrogen peroxide sensor, Sens. Actuators, A 134 (2007) 146–151.
[17] A. Primo, T. Marino, A. Corma, R. Molinari, H. García, Efficient visible-light photocatalytic water splitting by minute amounts of gold supported on nanoparticulate $CeO_2$ obtained by a biopolymer templating method, J. Am. Chem. Soc. 133 (2011) 6930–6933.
[18] X.M. Li, L. Sun, A.Q. Ge, Y.S. Guo, Enhanced chemiluminescence detection of thrombin based on cerium oxide nanoparticles, Chem. Commun. 47 (2011) 947–949.
[19] J.Z. Wang, C. Zhong, S.L. Chou, H.K. Liu, Flexible free-standing graphene–silicon composite film for lithium-ion batteries, Electrochem. Commun. 12 (2010) 1467–1470.
[20] Y. Wang, Y. Shao, D.W. Matson, J.H. Li, Y.H. Lin, Nitrogen-doped graphene and its application in electrochemical biosensing, ACS Nano 4 (2010) 1790–1798.
[21] Y. Wang, C.X. Guo, J.H. Liu, T. Chen, H.B. Yang, C.M. Li, $CeO_2$ nanoparticles/graphene nanocomposite-based high performance supercapacitor, Dalton Trans. 40 (2011) 6388–6391.
[22] S. Brahim, D. Narinesingh, A. Guiseppi-Elie, Amperometric determination of cholesterol in serum using a biosensor of cholesterol oxidase contained within a polypyrrole–hydrogel membrane, Anal. Chim. Acta 448 (2001) 27–36.

[23] C.Z. Zhao, L. Wan, L. Jiang, Q. Wang, K. Jiao, Highly sensitive and selective cholesterol biosensor based on direct electron transfer of hemoglobin, Anal. Biochem. 383 (2008) 25–30.
[24] A.L. Gopalan, K.P. Lee, D. Ragupathy, Development of a stable cholesterol biosensor based on multi-walled carbon nanotubes–gold nanoparticles composite covered with a layer of chitosan–room-temperature ionic liquid network, Biosens. Bioelectron. 24 (2009) 2211–2217.
[25] R. Manjunatha, D.H. Nagaraju, G.S. Suresh, J.S. Melo, S.F. D'Souza, T.V. Venkatesha, Direct electrochemistry of cholesterol oxidase on MWCNTs, J. Electroanal. Chem. 651 (2011) 24–29.